# Coherent combining of multiple beams with multi-dithering technique: 100KHz closed-loop compensation demonstration

Ling Liu[a], Dimitrios N. Loizos[b]
Mikhail A. Vorontsov[ac], Paul P. Sotiriadis[b], Gert Cauwenberghs[d]

[a]Intelligent Optics Laboratory, Institute for Systems Research, University of Maryland
College Park, MD 20742, U.S.A
[b]Department of Electrical and Computer Engineering, The Johns Hopkins University
Baltimore, MD 21218, U.S.A
[c]Computational and Information Sciences Directorate, Army Research Laboratory
2800 Powder Mill Road, Adelphi, MD 20783, U.S.A
[d]Division of Biological Sciences, University of California
San Diego, CA 92093, U.S.A

## Abstract

We demonstrate the coherent combining of three beams with a phase-locking controller using VLSI multi-dithering technique. Three fiber-coupled phase shifters are used to compensate phase distortions in the beam propagation path. The highest dither frequency in our system is ∼70MHz. The achieved closed-loop compensation bandwidth of three beamlets is up to 100KHz.

Keywords: coherent beam combining, phase-locking, multi-dithering

## 1. Introduction

Coherent beam combining is an important research area for laser communications and beam projection applications. The reported experimental demonstrations from other research groups are briefly described as follows. In [1–3], a phase-compensating 70-mm-diameter aperture transceiver with a hexagonal closely-packed array of seven 23-mm-diameter fiber collimator sub-apertures was demonstrated. The signal at the far field receiver was maximized by modulating each sub-aperture's phase through adjusting the pump current to its amplifier's pump diode using multi-dithering control with lock-in amplifier. The dither frequency is about 20KHz. The feedback signal was acquired from the photo detector at the target plane in the concave-mirror-converted far field. In [4], the optical outputs from 48 polarization maintaining fibers in an 8×8 fiber array (only 48 were used) with $250\mu$m pitch were collimated through an 8×8 lenslet array with the same pitch. The 48 collimated micro-beams were coherently combined through modulating individual in-line phase modulators (piezo stretchers) using stochastic parallel gradient descent method. The update rate of the controller is about 8KHz iterations per second. The feedback signal was acquired from the photo detector at the target plane in convex-lens-converted far field. In both systems, the compensation effects for the phase distortions along the propagation path were demonstrated. However, the speed of the phase-locking controller are not very fast in these two systems. As a part of the research efforts for the conformal adaptive phase-locked fiber collimator array [5], the coherent beam combining using multi-dithering technique is demonstrated in this paper. The coherent beam combining using stochastic parallel gradient descent techniques for the conformal optical system is presented separately in [6].

## 2. Experimental Setup

The real far field distance is too large (up to a few kilometers) to do the experiments in the laboratory. A far field conversion lens is used to simulate the far field in our experiments. A picture of the experimental optical setup with a three-element conformal optical transmitter in the laboratory is given in figure 1. The red arrowed lines show the propagation paths of the three beamlets.
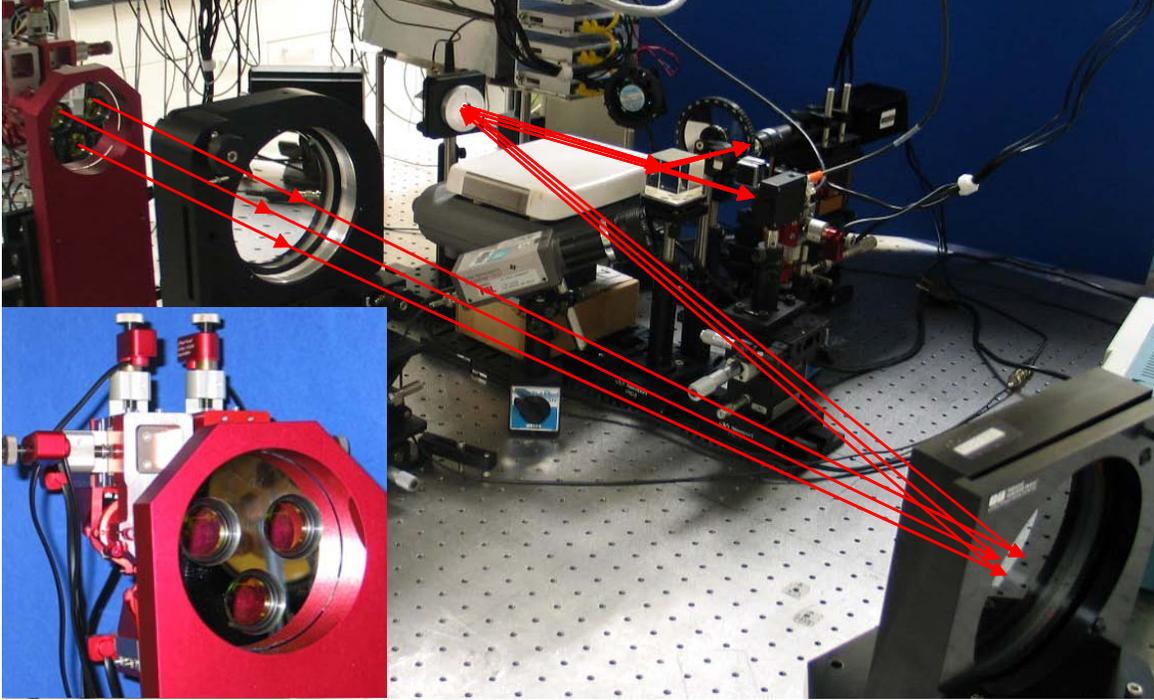
Figure 1: Experimental optical setup with three-element transmitter. The red arrowed lines show the propagation paths of the beamlets. Transmitter with three sub-apertures. Equivalent conformal aperture diameter $D \approx 71$mm. Sub-aperture lens diameter $d$=25mm. Sub-aperture lens focal length $f$=107mm. Distance between lens centers $l$=40mm. Wavelength $\lambda$=1060nm. Whole conformal aperture fill-factor is $\sim 0.37$. Sub-aperture beamlet fill-factor is $\sim 0.75$. The hotplate (in white) between the tip-tilt mirror and the cubic beam splitter is used to generate phase distortions. A cooling fan is used to generate airflow. For convenience, the upper-right sub-aperture (beamlet) is identified as #1, the upper-left sub-aperture (beamlet) is identified as #2, and the bottom sub-aperture (beamlet) is identified as #3.

In order to coherently combine the three beamlets in the far field, we prepare the beamlets as follows. The three quasi-monochromatic beamlets are collimated at the transmitter pupil plane. The three collimated beamlets are aligned in parallel to each other so that they can be combined and focused in the same target focal plane in the far field. The three beamlets are generated by splitting a beam from a single seed laser into a few parts which are correlated in phase to each other. The length differences of three fiber optical paths are controlled to be smaller than the coherence length of the laser source. The three beamlets are linearly polarized. Their polarization angles are matched.

More specifications of the experimental setup are given in figure 2. A fiber-coupled diode laser with wavelength 1060nm is used in the experiments. The laser output has a linewidth of $\sim 300$KHz and a coherence length of $\sim 700$m. The length differences between the fiber optical paths ($\sim 10$m) for each beamlet are <0.5m which is much smaller than the coherence length of the seed laser. The three outgoing beamlets into the free space are correlated in phase after passing through the optical fiber paths. The output power grating of the used diode seed laser is $\sim 150$mW.

All the optical fibers used in the experiments are Panda type polarization-maintaining single-mode fibers with the design wavelength $\lambda$=1060nm. All the fiber connectors are FC/APC in order to reduce the back-reflections in the fiber-to-fiber couplings. The polarization-maintaining fiber beam splitter has built-in phase shifters and amplitude controls. Each phase shifter need a control voltage (denoted by $U1$, $U2$ and $U3$) $\sim 2.2$V to generate a $\pi$-radian phase shift. The active waveguide of the Mach-Zehnder interferometer for the amplitude control need

a control voltage (denoted by $A1$, $A2$ and $A3$) $\sim$4.1V to tune the beamlet power from its maximum value to zero. The amplitude control voltages ($U1$, $U2$ and $U3$) are tuned to appropriate DC values (usually $\pm0.5$V) in order to balance the powers of the three beamlets. The phase shifts for the three beamlets are modulated by the control voltages generated by the multi-dithering phase-locking controller.

There are three polarization-maintaining fiber-coupled beam collimators for the three beamlets, respectively. The three beam collimators are used to collimate the three beamlets, to align them in parallel to each other and to couple them into the free space. The three collimated beamlets in parallel pass the far field conversion lens, and are reflected by a large plane mirror and then are reflected again by a small plane mirror, to a polarization-independent cubic beam splitter. After the cubic beam splitter, part of the beam is transmitted to the target pinhole (diameter $50\mu$m) and part of the beam is reflected through an attenuator wheel to the microscope-coupled CCD focused at the target focal plane. A photo detector (PDA-10CF, 150MHz bandwidth) and a wideband amplifiter (DHPVA-100, 100MHz bandwidth, 10-60dB gain) are located immediately behind the target pinhole. The bandwidth of the combo of the given photo detector and the amplifier is from DC to 100MHz for the used wavelenth $\lambda = 1060$nm. The collected power (denoted by $J$) by the pinhole is used as the feedback input signal by the multi-dithering phase-locking controller. This feedback signal is our system metric to be maximized. The three beamlets propagate in free space from the transmitter pupil to the target pinhole. In this propagation path, wavefront phase distortions can be introduced with the hotplate and the cooling fan as shown in figure 1.

## 3. Multi-dithering controller for phase-locking

Multi-dithering algorithm[7,8] is a commonly used technique for the phase-locking control in coherent beam combining[2,3,9]. In our system, phase-locking control is implemented with a mixed-signal VLSI multi-dithering controller[10] as shown in figure 3. The multi-dithering algorithm implemented on this specific controller is described as follows.

There are eight parallel control channels available in our multi-dithering controller. We have three beamlets in our experiments. In total, we need to use three control channels to apply three voltages (denoted by $U_i(t)$, $i = 1, 2, 3$) to the three fiber phase shifters for phase-locking control.

For convenience, we use the following convention in this section. $\{\cdot\}$ represents the ensemble of variables with the general indicator enclosed by $\{\}$. For example, $U_i(t)$ is a single control voltage, while $\{U_i(t)\}$ indicates the ensemble $\{U_1(t), U_2(t), U_3(t)\}$.

The system metric $J$ can be written as a function of the control voltages

$$J \equiv J(\{U_i(t)\}) \tag{1}$$

The phase-locking control using multi-dithering technique can be realized by updating the control voltages $\{U_i(t)\}$ continuously with estimating their gradients in the following manner. For a given $i = 1, 2, 3$

$$\frac{dU_i(t)}{dt} = \gamma \overline{\langle J(\{U_j(t) + \alpha_j \cos(\omega_j t)\}) \cos[\omega_i(t + T) + \psi_i]\rangle}_{LPBW} \tag{2}$$

where

$$LPBW = \min\{|\omega_i - \omega_j|\}, \quad \text{for} \quad 1 \leqslant i \neq j \leqslant 3 \tag{3}$$

is the cutoff frequency of the lowpass operation denoted by $\overline{\langle\cdot\rangle}_{LPBW}$, $\gamma$ is the update gain for all the control voltages $\{U_i(t)\}$, $\{\alpha_i\}$ are the respective small amplitudes of the harmonic dithers $\{\alpha_i \cos(\omega_i t)\}$ for the control voltages $\{U_i(t)\}$, $\{\omega_i\}$ are the respective frequencies of the harmonic dithers $\{\alpha_i \cos(\omega_i t)\}$ for the control voltages $\{U_i(t)\}$, $T$ is defined as the total time delay between the instant at which the dithers are applied to the control voltages $\{U_i(t)\}$ and the instant at which the metric $J$ is picked up by the multi-dithering controller to do the above lowpass evaluation, $\{\cos(\omega_i t + \psi_i)\}$ are phase-shifted harmonic signals, $\{\psi_i\}$ are the relative phase shifts of the phase-shifted harmonic signals.

Laser (1060 nm)

PM Fiber

Mating Sleeve

PM Fiber Beam Splitter with Phase Shifter & Amplitude Controls

U1  U2  U3

A1  A2  A3

PM Fiber

Mating Sleeve

Static Amplitude Controls

U1  U2  U3

A1  A2  A3

Mixed-signal VLSI Multi-dithering Phase-locking Controller

Metric J

Received Power (Metric J)

Beam Collimator

Lens ( f = 107 mm )

Lens ( f = 1900 mm )

30 cm

65 cm

83 cm

Mirror

Mirror

Target Focal Plane

Attenuator

BS

Microscope with CCD and Filter (1060 nm)

42 cm

Received Power (Metric J)

Target Pinhole (50μm)
Photo Detector (PDA-10CF)
Wideband Amp. (DHPVA-100)

Figure 2: Schematic of experimental setup

Figure 3: VLSI multi-dithering controller developed at the Johns Hopkins University (2006). Dither frequency range: 100Hz~800MHz. Channel output dynamic range: 0.5~2.5V. The IDC50 connector is for interfacing to PC card (PCI-DAC6703). Power supplies are 0.0~+3.0V. There are eight output channels and each channel has two output terminals with 50Ω output impedance. There are two differential metric inputs terminals with 50Ω input impedance.

Here $LPBW$ is assumed to be less than the minimum value of $\{\omega_i\}$. The selection of the lowpass cutoff frequency $LPBW$ depends on the frequency spectrum of the phase noises to be compensated. If the $LPBW$ is known, then the dither frequencies $\{\omega_i\}$ can be selected. Without consideration for the time delay $T$, the above evaluation of the gradients cannot be performed synchronously in the real-time control system.

With proper selections of $\{\psi_i\}$ and positive update gain $\gamma$, the system metric $J$ can be (locally) maximized. This can be verified briefly as follows. If the dithers $\{\alpha_i \cos(\omega_i t)\}$ are applied to the control voltages $\{U_i(t)\}$ at the instant $t$, then the following detection of the system metric $J\left(\{U_j(t) + \alpha_j \cos(\omega_j t)\}\right)$ is performed at the instant $t + T$.

$$J\left(\{U_j(t) + \alpha_j \cos(\omega_j t)\}\right) = J\left(\{U_j(t)\}\right) + \sum_{j=1}^{3} \alpha_j \frac{\partial J}{\partial U_j} \cos(\omega_j t) + o(\{\alpha_j\}) \tag{4}$$

where $o(\{\alpha_j\})$ means the higher order ($\geq 2$) terms of $\{\alpha_j\}$.

$J\left(\{U_j(t) + \alpha_j \cos(\omega_j t)\}\right)$ and $\{\cos[\omega_i(t+T) + \psi_i]\}$ are synchronous in real-time multi-dithering controller. With a little algebra, the lowpass operation for a given $i = 1, 2, 3$ gives

$$\overline{\langle J\left(\{U_j(t) + \alpha_j \cos(\omega_j t)\}\right) \cos[\omega_i(t+T) + \psi_i]\rangle}_{LPBW} = \frac{\alpha_i}{2} \frac{\partial J}{\partial U_i} \cos(\omega_i T + \psi_i) \tag{5}$$

We have

$$\frac{dU_i(t)}{dt} = \frac{1}{2}\gamma \alpha_i \frac{\partial J}{\partial U_i} \cos(\omega_i T + \psi_i) \tag{6}$$

$$\frac{dJ\left(\{U_i(t)\}\right)}{dt} = \sum_{i=1}^{3} \frac{\partial J}{\partial U_i} \frac{dU_i(t)}{dt} = \frac{1}{2}\sum_{i=1}^{3} \gamma \alpha_i \left(\frac{\partial J}{\partial U_i}\right)^2 \cos(\omega_i T + \psi_i) \tag{7}$$

Assume update gain coefficient $\gamma$ and all small dither amplitudes $\{\alpha_i\}$ are positive. As long as the roundtrip time delay $T$ is known, $\{\psi_i\}$ can be selected such that $\{\cos(\omega_i T + \psi_i)\}$ are non-negative. This makes $\frac{dJ(\{U_i(t)\})}{dt} \geq 0$, which indicates a (locally) maximizing process for the system metric $J$. Usually it is difficult to detect $T$ directly in the real-time control system. A trial-and-error method is used to select each $\psi_i$ from a set of discrete values $\left\{0, \frac{\pi}{3}, \frac{2\pi}{3}, \pi, \frac{4\pi}{3}, \frac{5\pi}{3}\right\}$.

In general, the selection results of $\{\psi_i\}$ in the above trial-and-error scheme are not unique. Different selections of $\{\psi_i\}$ give different absolute values of $\frac{dJ(\{U_i(t)\})}{dt}$. This affects the convergence speed of the system metric $J$. The convergence speed is also dependent on the selections of the update gain coefficient $\gamma$ and the dither amplitudes $\{\alpha_i\}$. Appropriately increasing $\gamma$ and $\{\alpha_i\}$ can increase the convergence speed of the system metric $J$.

## 4. Experimental Results

Figure 4 shows the target plane intensity distributions for incoherent beam combining and coherent beam combining. The beamlet identifications are defined in figure 1. In the pseudo-incoherent beam combining, the phases of the three beamlets are scrambled to be random enough by the fiber phase shifters to which three sinusoidal voltages with different high frequecies (>1MHz) and high amplitudes (>2π-radian phase shift) are applied. In the coherent beam combining cases, the phase-locking control is on. There is only static or quasi-static phase distortions due to the fiber optical path length differences between the three channels, fiber optical path length slow variations and so on. There are not any fast varying phase distortions or jitters present in the propagation path of the beamlets. The images are the time-averaged (instead of instantaneous) intensity distributions seen on the monitor due to the finite response time of the CCD camera. It is not difficult to understand the images (a-e). For these five cases, the instantaneous intensity distributions have the similar patterns as to the respective averaged distibutions here. In the case (f) for the coherent beam combining by destructive phase-locking, the control system tries every effort to minimize the received power in the pinhole. The central lobe (brightest spot) of the combined beam can be anywhere around the pinhole. This is the instantaneous case. On average, a dark hole and a bright ring are seen on the image (f). The central dark hole is not surrounded by a uniform bright ring in the image (f) because the integration time of the camera is not long enough. The scale 50$\mu$m is shown because the it is equal to the pinhole diameter. There are strong side lobes present in these images. The strong side lobes are due to the relatively small conformal fill factor 0.37 of the conformal transmitter with three sub-apertures.

The phase-locking compensation power using fiber phase shifters with our multi-dithering controller is characterized in the following two experiments. All the beamlets are aligned in parallel to each other. The powers of the three beamlets are balanced using the built-in amplitude controls inside the fiber phase shifters. In the characterizing procedure, high frequency phase distortions are simulated by applying a harmonic voltage to one of the phase shifters in use. This is because the phase distortions generated through the hotplate and the cooling fan has only low frequency (<100Hz) components. Phase distortions up to 400KHz is introduced to one beamlet relative to the others. There are no phase distortions introduced by the hotplate and the cooling fan or jitters. These two experiments are described as follows.

Phase-locking of two beamlets (#1 and #2) using the multi-dithering controller is performed. Beamlet #3 is blocked. The phase of beamlet #1 is distorted by applying a sinusoidal voltage to the phase control electrode of fiber phase shifter #1. The phase of beamlet #2 is controlled by one channel output of the multi-dithering controller. The distortion phase-shift amplitude and the compensation bandwidth are recorded. Here the phase-locking compensation bandwidth for a given distortion phase-shift amplitude is defined as the cutoff frequency (the highest frequecy of the sinusoidal distorting voltage) at which the normalized metric is 0.85. The normalized metric in a phase-locking state is calculated by dividing the averaged metric signal when distortion is present by the averaged metric signal when distortion is absent. This experiment corresponds to the curve in red in figure 5.
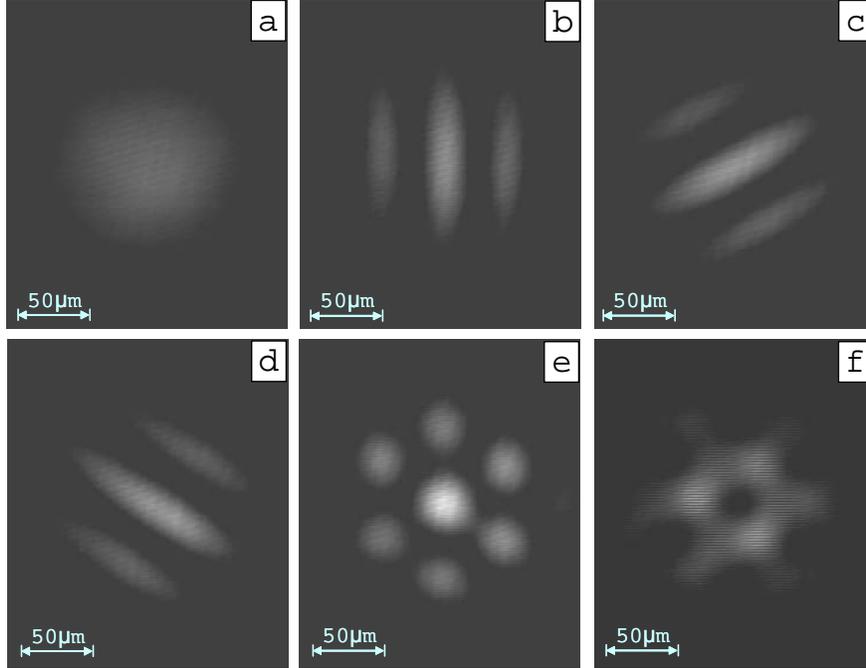
Figure 4: Target plane intensity distributions for incoherent beam combining and coherent beam combining. (a) incoherent combining of three beamlets, (b) coherent combining of two beamlets (#1 and #2), (c) coherent combining of two beamlets (#2 and #3), (d) coherent combining of two beamlets (#1 and #3), (e) coherent combining of three beamlets (constructively phase-locked), (f) coherent combining of three beamlets (destructively phase-locked). The images are the time-averaged (instead of instantaneous) intensity distributions seen on the monitor due to the finite response time of the CCD. The beamlet identifications are defined in figure 1.

Phase-locking of three beamlets using the multi-dithering controller is performed. The phase of beamlet #1 is distorted by applying a sinusoidal voltage to the phase control electrode of fiber phase shifter #1. The phases of the other two beamlets (#2 and #3) are controlled by two channel outputs of the multi-dithering controller. The distortion phase-shift amplitude and the compensation bandwidth are recorded. This experiment corresponds to the curve in blue in figure 5.

In the above experiments, the highest dither frequency is ∼70MHz and the lowpass cutoff frequency $LPBW$ is set to be ∼4.7MHz. Figure 5 shows that the compensation bandwidth for phase-locking of two beamlets is generally higher than the compensation bandwidth for phase-locking of three beamlets for a given distortion phase-shift amplitude. The phase-locking of more beamlets are more difficult than the phase-locking of less beamlets in general.

The transition process from phase-unlocked state to phase-locked state using VLSI multi-dithering phase-locking controller is investigated. Here phase-unlocked state means the state where phase-locking control is off when the atmospheric phase distortions generated by the hotplate and the cooling fan are present. The phase-locked state means the stable convergence state when the same atmospheric phase distortions are present. The three beamlets are combined together and are modulated by the respective fiber phase shifters. The transition process is defined starting at the moment when the control systems are turned on and ending at the moment the normalized metric reaches 95% of the value of its stable convergence state. This is shown in figure 6. This plot is obtained on an oscilliscope automatically because the data acquisiton board PCI-DAS1602/12 for metric signal is not able to sample the metric fast enough. The convergence time is ∼1.90µs. The needed number of dither cycles is 133 for 3 beamlets. The system needs 44 dither cycles per beamlet to converge to its stable state.
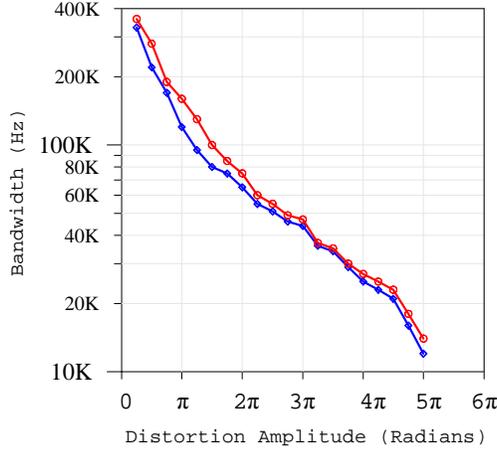
Figure 5: Phase-locking compensation power using multi-dithering controller. These curves correspond to the normalized metric 0.85. The highest dither frequency is ∼70MHz. The curve in red is for the phase-locking of two beamlets (#1 and #2). The curve in blue is for the phase-locking of three beamlets. In each case, the distortion is generated by applying a sinusoidal voltage to the phase modulating terminal of the fiber phase shifter #1. No jitters or atmospheric phase distortions are present.
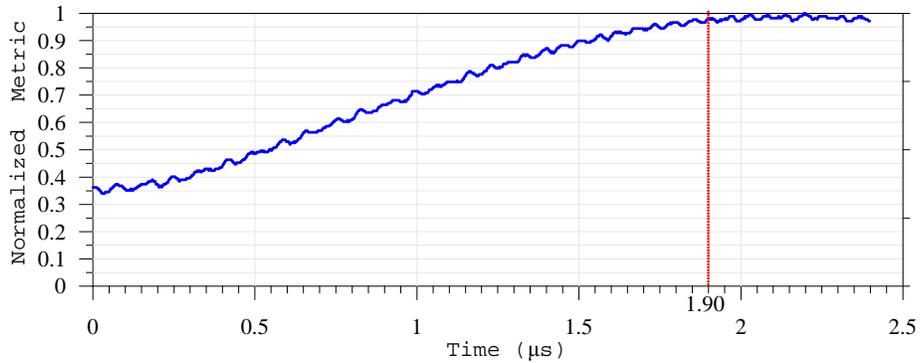


Figure 6: Phase-locking transition curve using the VLSI multi-dithering controller. The highest dither frequency is ∼70MHz. The convergence time is $1.90\mu s$. The needed number of dither cycles for convergence is 133 for 3 beamlets. Atmospheric phase distortions generated by the hotplate and the cooling fan are present. No jitters are present. The ripples on the curve are due to the $2\pi$-jumps of the multi-dithering controller. (see [10])

## 5. Summary

We have experimentally demonstrated the coherent combining of three collimated beamlets with a multi-dithering phase-locking controller based on mixed-signal VLSI technology. The highest dither frequency used in our system is ∼70MHz. The compensation bandwidth for phase distortions is up to 100KHz when the distortion amplitude corresponds to about $\pi$-radian phase shift. However, the current implementation of the VLSI multi-dithering controller need be further improved in the following aspect. The trial-and-error selection method for $\{\psi_i\}$ as described in the controller section need be replaced with an automatic selection method.

# References

[1] M. Minden, "Coherent Coupling of a Fiber Amplifier Array," in 13th Annual Solid State and Diode Laser Technology Review, SSDLTR 2000, Tech. Digest (Air Force Research Laboratory, Albuquerque, N.M. 2000).

[2] M. Mangir, H. Bruesselbach, M. Minden, S. Wang and C. Jones, "Atmospheric Aberration Mitigation and Transmitter Power Scaling Using a Coherent Fiber Array," Proc. of 2004 IEEE Aerospace Conference.

[3] H. Bruesselbach, S. Wang, M. Minden, D. C. Jones and M. Mangir, "Power-Scalable Phase-Compensating Fiber-Array Transceiver for Laser Communications through the Atmosphere," J. Opt. Soc. Am. B, V.22, 2005.

[4] J. E. Kansky, C. X. Yu, D. V. Murphy, S. E.J. Shaw, R. C. Lawrence and C. Higgs, "Beam Control of a 2D Polarization Maintaining Fiber Optic Phased Array with High-Fiber Count," Proc. of SPIE V. 6306, 2006.

[5] M. A. Vorontsov, "Adaptive Photonics Phase-Locked Elements (APPLE): System Architecture and Wavefront Control Concept," Proc. of SPIE V. 5895, 2005.

[6] L. Liu, M. Vorontsov, E. Polnau, T. Weyrauch and L. Beresnev, "Adaptive Phase-Locked Fiber Array with Wavefront Tip-Tilt Compensation," Proc. of SPIE V. 6708, 2007.

[7] J. W. Hardy, "Adaptive optics: a new technology for the control of light," Proc. IEEE 66, 651-697 (1978).

[8] T. R. O'Meara, "The multi-dither principle in adaptive optics," J. Opt. Soc. Am. 67, 306-315 (1977).

[9] M. A. Vorontsov, "Chapter 7: Wavefront Control Algorithms," (from the manuscript of the book: "Wavefront Controller in Optics").

[10] D. Loizos, L. Liu, P. Sotiriadis, G. Cauwenbergs, M. Vorontsov, "Integrated Multi-Dithering Controller for Adaptive Optics," Proc. of SPIE V. 6708, 2007.